Journal of Environmental Management 91 (2010) 1456–1466

Contents lists available at ScienceDirect

Journal of Environmental Management

journal homepage: www.elsevier.com/locate/jenvman

Three-dimensional numerical simulation of water quality and sediment-associated processes with application to a Mississippi Delta lake

Xiaobo Chao [a,*], Yafei Jia [a], F. Douglas Shields Jr. [b], Sam S.Y. Wang [a], Charles M. Cooper [b]

[a] National Center for Computational Hydroscience and Engineering, University of Mississippi, Carrier Hall 102, University, MS 38677, USA
[b] National Sedimentation Laboratory, U. S. Department of Agriculture, Agricultural Research Service, P.O. Box 1157, Oxford, MS 38655, USA

ARTICLE INFO

Article history:
Received 8 October 2008
Received in revised form
17 September 2009
Accepted 9 February 2010
Available online 15 March 2010

Keywords:
Water quality model
Sediment
Phytoplankton
Nutrients, Oxbow lake

ABSTRACT

A three-dimensional water quality model was developed for simulating temporal and spatial variations of phytoplankton, nutrients, and dissolved oxygen in freshwater bodies. Effects of suspended and bed sediment on the water quality processes were simulated. A formula was generated from field measurements to calculate the light attenuation coefficient by considering the effects of suspended sediment and chlorophyll. The processes of adsorption–desorption of nutrients by sediment were described using the Langmuir Equation. The release rates of nutrients from the bed were calculated based on the concentration gradient across the water–sediment interface and other variables including pH, temperature and dissolved oxygen concentration.

The model was calibrated and validated by applying it to simulate the concentrations of chlorophyll and nutrients in a natural oxbow lake in Mississippi Delta. The simulated time series of phytoplankton (as chlorophyll) and nutrient concentrations were generally in agreement with field observations. Sensitivity analyses were conducted to demonstrate the impacts of varying suspended sediment concentration on lake chlorophyll levels.

© 2010 Elsevier Ltd. All rights reserved.

1. Introduction

Sediment has been identified as one of the leading nonpoint source pollutants in the United States. Sediments are associated with nutrients and pesticides, and greatly affect water quality. Suspended sediment (SS) reduces light intensity, which is one of the most important factors to the growth of phytoplankton. Nutrients and pesticides adsorb to sediment particles and also desorb from sediment to the water. In addition, nutrients adsorbed to bed sediments may be released back into the water column. Sediment-associated processes that need to be considered in water quality studies include the effect of sediment on light intensity, the adsorption–desorption of nutrients by sediment, and the exchange of water quality constituents between the bed sediment layer and water column.

Studying water quality problems in the natural environment with numerical models is a very effective approach. Many numerical models for simulating water quality processes have been developed (Cerco and Cole, 1995; Jin et al., 1998; Gin et al., 2001; Wool et al., 2001; Kuo et al., 2008). Some well-established three-dimensional models, such as WASP6 (Wool et al., 2001), CE-QUAL-ICM (Cerco and Cole, 1995), Delft3D-WAQ (Delft Hydraulics, 2003), MIKE3_WQ (Danish Hydraulic Institute, 2005), ECOM/RCA (Hydroqual, 2004), etc., have been used to simulate water quality variables in rivers, lakes, estuaries and coastal waters. Some successful applications of numerical models for the study of water quality constituents in natural water bodies have been reported (Dortch et al., 2008; Chung et al., 2008; Fan et al., 2009). These published models generally simulate basic physical, chemical and biological processes of aquatic ecosystems. However, only a few are capable of simulating the effects of sediment on water quality. The processes of adsorption–desorption and release of nutrients from bed sediment were considered in WASP6, CE-QUAL-ICM, and Delft3D-WAQ. In these models, the release rate of nutrients from the bed sediment was determined using functions of the concentration gradient across the water–sediment interface; however, the effects of pH and dissolved oxygen (DO) concentration on the release rate were not considered. In WASP6 and CE-QUAL-ICM, the adsorption–desorption of nutrients by sediment were described using a linear approach. In WASP6, the effect of SS concentration on the growth of phytoplankton was not taken into account.

A three-dimensional water quality model was developed to predict the concentrations of phytoplankton, nutrients and DO. This model was decoupled with a three-dimensional free surface hydrodynamics model CCHE3D (Jia et al., 2001), and the major

* Corresponding author. Tel.: +1 662 915 6564; fax: +1 662 915 7796.
E-mail address: chao@ncche.olemiss.edu (X. Chao).

0301-4797/$ – see front matter © 2010 Elsevier Ltd. All rights reserved.
doi:10.1016/j.jenvman.2010.02.009

sediment-associated processes (e.g., the effect of sediment on light intensity, the adsorption–desorption of nutrients by sediment and the release of nutrients from bed sediment) were included. This model was calibrated and validated by applying it to simulate the concentration of nutrients and chlorophyll in a natural oxbow lake receiving runoff from an intensively cultivated watershed in Mississippi Delta.

2. Water quality processes considered in the numerical model

2.1. Basic processes

In the water quality model, four biochemical processes were selected for modeling: the phytoplankton kinetics, nitrogen cycle, phosphorus cycle, and DO balance. The conceptual framework for the eutrophication kinetics in the water column was mainly based on the WASP6 model (Wool et al., 2001). Eight state variables were involved in the interacting systems: ammonia nitrogen (NH_3), nitrate nitrogen (NO_3), phosphate (PO_4), phytoplankton (PHYTO), carbonaceous biochemical oxygen demand (CBOD), DO, organic nitrogen (ON), and organic phosphorus (OP).

2.1.1. Phytoplankton kinetics

Phytoplankton, a group of microscopic plants that live in water, plays a central role in the carbon and nutrient cycles that comprise the model ecosystem. During photosynthesis, phytoplankton use nutrients (e.g., inorganic carbon, nitrogen and phosphorus) and energy from light to produce organic compounds, releasing oxygen as a by-product. In the model, total chlorophyll is used as a simple measure of phytoplankton biomass, and the source term due to phytoplankton growth and death is calculated by

$$\sum S_{\mathrm{chl}} = (G_{\mathrm{p}} - D_{\mathrm{p}} - P_{\mathrm{set}})C_{\mathrm{chl}} \tag{1}$$

in which $\sum S_{\mathrm{chl}}$ is the effective source term for phytoplankton; G_{p} is the growth rate of phytoplankton (day^{-1}); D_{p} is the death rate of phytoplankton (day^{-1}); P_{set} is the effective phytoplankton settling rate (day^{-1}); and C_{chl} is the concentration of chlorophyll (mg/l).

The growth rate of phytoplankton is determined by the availability of nutrients, the intensity of light, and the ambient temperature. The effects of each factor are considered to be multiplicative:

$$G_{\mathrm{p}} = P_{\mathrm{mx}} f_{\mathrm{N}} f_{\mathrm{I}} f_{\mathrm{T}} \tag{2}$$

in which f_{N}, f_{I} and f_{T} are the limitation factors due to nutrient availability, light intensity, and temperature, respectively; P_{mx} is the maximum phytoplankton growth rate (day^{-1}).

f_{N} is calculated based on Michaelis–Menten Equation and Liebig's law of the minimum (Cerco and Cole, 1995; Wool et al., 2001):

$$f_{\mathrm{N}} = \min\left(\frac{C_{\mathrm{NH3}} + C_{\mathrm{NO3}}}{C_{\mathrm{NH3}} + C_{\mathrm{NO3}} + K_{\mathrm{mN}}}, \frac{C_{\mathrm{PO4}}}{C_{\mathrm{PO4}} + K_{\mathrm{mP}}}\right) \tag{3}$$

in which C_{NH3}, C_{NO3} and C_{PO4} are the concentration of NH_3, NO_3 and PO_4, respectively (mg/l); K_{mN} and K_{mP} are the half-saturation constants for nitrogen and phosphorus uptake, respectively(mg/l).

f_{I} is calculated by integrating the Steele equation over water depth and time (Chapra, 1997):

$$f_{\mathrm{I}} = \frac{2.72 f_{\mathrm{d}}}{K_e \Delta z}\left[\exp\left(-\frac{I_0}{I_{\mathrm{m}}} e^{-K_e(zd+\Delta z)}\right) - \exp\left(-\frac{I_0}{I_{\mathrm{m}}} e^{-K_e \cdot zd}\right)\right] \tag{4}$$

in which f_{d} is the photoperiod; Δz is the thickness of model segment (m); zd is the distance from the water surface to the top level of a computational element in the water (m); K_{e} is the total light attenuation coefficient (m^{-1}), in this model, the effect of suspended sediment on the f_{I} is considered; I_0 is the daily light intensity at the water surface (ly/day); I_{m} is the saturation light intensity of phytoplankton (ly/day).,

f_{T} is obtained using formulas proposed by Cerco and Cole (1995):

$$f_{\mathrm{T}} = \exp\left[-KTg_1(T - T_{\mathrm{m}})^2\right] \quad \text{when } T \le T_{\mathrm{m}} \tag{5}$$

$$f_T = \exp\left[-KTg_2(T_m - T)^2\right] \quad \text{when } T > T_{\mathrm{m}} \tag{6}$$

in which T is the temperature (°C); T_{m} is the optimal temperature for phytoplankton growth(°C); KTg_1 and KTg_2 are coefficients representing the effects of temperature on growth below and above T_{m}, respectively.

2.1.2. Nutrient cycles

In this model, nutrient cycles include the nitrogen cycle and the phosphorus cycle. In the nitrogen cycle, ammonia (NH_3) and nitrate (NO_3) are consumed by phytoplankton (PHYTO) for growth. For physiological reasons, NH_3 is the preferred form of inorganic nitrogen for phytoplankton. Nitrogen is returned from the phytoplankton biomass pool to particulate and dissolved organic nitrogen (ON) pools as a result of death and endogenous respiration of phytoplankton and grazing and mortality of zooplankton. Organic nitrogen is converted to NH_3 at a temperature-dependent mineralization rate, and NH_3 is then converted to NO_3 at a temperature- and oxygen-dependent nitrification rate. In the absence of oxygen, NO_3 can be converted to nitrogen gas (denitrification) at a temperature-dependent rate.

Phosphorus kinetics is similar to the nitrogen kinetics except there is no process analogous to denitrification. Inorganic phosphorus (PO_4) is utilized by phytoplankton (PHYTO) for growth and is incorporated into phytoplankton biomass. Phosphorus is returned to the water column from dead or decaying phytoplankton biomass in the bed. The various forms of organic phosphorus (OP) undergo settling, hydrolysis and mineralization, and are converted to inorganic phosphorus at temperature-dependent rates.

2.1.3. DO balance

Dissolved oxygen is one of the most important variables in water quality analysis. The sources of DO included in the model are reaeration, photosynthetic oxygen production, and DO in inflows. The sinks of DO include phytoplankton respiration, oxidation of carbonaceous biochemical oxygen demand (CBOD), nitrification and sediment oxygen demand (SOD).

2.2. Sediment-associated water quality processes

Suspended sediment reduces light penetration (Stefan et al., 1983). This reduces phytoplankton growth by limiting the amount of solar energy available for photosynthesis. The processes of adsorption–desorption of nutrients by suspended sediment are also important for the fate and transport of nutrients. In addition, DO and nutrients may move between the bed sediment layer and water column. In this study, the effect of groundwater on the bed exchange was not taken into account, so the exchange of DO or nutrients was primarily dominated by the diffusion at the interface of bed sediment and water column. To model these complex processes, the effects of sediment on the phytoplankton growth, nutrients and DO were considered in the proposed water quality model.

2.2.1. Effect of sediment on phytoplankton growth

The light attenuation coefficient K_e in Eq. (4) is determined by the effects of water, chlorophyll and SS, and can be expressed by (Stefan et al., 1983):

$$K_e = K_0 + K_{chl} + K_{ss} \tag{7}$$

where K_0 is the light attenuation by pure water (m^{-1}); K_{chl} is the attenuation by chlorophyll (m^{-1}); K_{ss} is the attenuation by SS (m^{-1}). Wool et al. (2001) proposed a formula to calculate K_e based on the light attenuation due to pure water and chlorophyll without consideration of the effect of SS:

$$K_e = K_0 + 0.0088C_{chl} + 0.054C_{chl}^{0.67} \tag{8}$$

in which C_{chl} is the concentration of chlorophyll (mg/l).

In fact, SS increases both water surface reflectivity and light attenuation. Field measurements by Stefan et al. (1983) showed attenuation by SS can be given by:

$$K_{ss} = \gamma s \tag{9}$$

where s is the concentration of suspended sediment; γ is a parameter obtained from field measurements. Combining Eqs. (8) and (9), Eq. (7) can be written as:

$$K_e = K_0 + 0.0088C_{chl} + 0.054C_{chl}^{0.67} + \gamma s \tag{10}$$

In this study, K_0 and γ were obtained based on field measurements.

2.2.2. The processes of adsorption–desorption

Dissolved nutrients may exchange between the water column and suspended sediment due to the processes of adsorption–desorption. Since the reaction rates for adsorption–desorption are much faster than those for biological kinetics, an equilibrium assumption can be made (Wool et al., 2001). In the numerical model, the processes of adsorption–desorption are assumed to reach equilibrium at each time step. In some models, the adsorption–desorption of nutrients by sediment was described by a linear isotherm, assuming a constant ratio of the equilibrium adsorption concentration to the dissolved nutrient concentration (Ishikawa and Nishmura, 1989; Wool et al., 2001). However, most experimental results show the Langmuir equilibrium isotherm is a better representation of the relations between the dissolved and particulate nutrient concentrations (Fox et al., 1989; Appan and Wang, 2000; Bubba et al., 2003). In this study, the Langmuir equation was adopted to calculate the adsorption and desorption rate. The equilibrium adsorption concentration Q (mg/mg SS) can be expressed as

$$Q = \frac{Q_m K C_d}{1 + K C_d} \tag{11}$$

where C_d is the dissolved nutrient concentration after the adsorption reaches equilibrium (mg/l); Q_m is the maximum adsorption capacity (mg/mg SS); and K is the ratio of adsorption and desorption rate coefficients (l/mg). It is assumed that the volume of the nutrient/water/sediment mixture is V_0, which is a constant in the adsorption–desorption processes. Let C_0 be the total initial nutrient concentration at each time step, and s be the sediment concentration (mg/l). Since the initial amount of nutrient in the mixture is same as when the adsorption reaches equilibrium, it can be expressed as Eq. (12):

$$C_0 V_0 = C_d V_0 + s V_0 Q. \tag{12}$$

so

$$C_d = C_0 - sQ \tag{13}$$

The particulate concentration C_p can be expressed as

$$C_p = sQ \tag{14}$$

By substituting Eqs. (13) and (14) into Eq. (11) and simplifying, a quadratic equation can be obtained:

$$C_p^2 - \left(\frac{1}{K} + C_0 + sQ_m\right)C_p + C_0 s Q_m = 0 \tag{15}$$

By using the quadratic formula, C_p and C_d can be solved as:

$$C_p = \frac{1}{2}\left[\left(C_0 + \frac{1}{K} + sQ_m\right) - \sqrt{\left(C_0 + \frac{1}{K} - sQ_m\right)^2 + \frac{4sQ_m}{K}}\right] \tag{16}$$

$$C_d = \frac{1}{2}\left[\left(C_0 - \frac{1}{K} - sQ_m\right) + \sqrt{\left(C_0 + \frac{1}{K} - sQ_m\right)^2 + \frac{4sQ_m}{K}}\right] \tag{17}$$

Eqs. (16) and (17) show the concentrations of particulate and dissolved nutrients due to adsorption–desorption are determined by the total initial concentration of nutrients C_0, the adsorption constants K and Q_m, and the suspended sediment concentration s. Since C_0 and s vary with time, the ratio of C_p and C_d is not a constant.

Eqs. (16) and (17) were tested using a laboratory experiment designed to study the adsorption capacities of ortho-phosphorus (Bubba et al., 2003). The experimental results show that the concentration of ortho-phosphorus in the liquid phase and the adsorption content can be described using Langmuir equilibrium equation, and the adsorption parameters K and Q_m were obtained. At equilibrium adsorption conditions, the concentrations of particulate and dissolved phosphate under different initial concentrations of 2.5, 5, 10, 20, and 40 mg/L were measured. Two stations' data were compared with calculations by Eqs. (16) and (17), and good agreements were obtained (Fig. 1a and b).

2.2.3. The exchanges of nutrients between bed sediment layer and water column

The diffusion model was adopted to quantify the exchange fluxes of nutrients at water–sediment interface. The exchange flux of nutrients S_c from bed sediment layer can be estimated using Fick's first law, which expresses that the flux is directly proportional to the concentration gradient and the porosity of sediment (Loeff et al., 1984; Moore et al., 1998; DiToro, 2001):

$$S_c = -\phi D_m \frac{dC}{dz} \approx \frac{\phi D_m}{\Delta z_b}(C_b - C_w) = k(C_b - C_w) \tag{18}$$

where S_c is the diffusive flux (mg/m^2/day); ϕ is the porosity of sediment; D_m is the molecular diffusivity (m^2/day); Δz_b is the diffusive sub-layer thickness near the bed (m); k is the diffusive exchange coefficient at water–sediment interface (m/day); C_w and C_b are the concentration of nutrients in water and water–sediment interface, respectively.

In the numerical model, the release rate of nutrients from the bed sediment layer is needed to calculate the source terms of nutrients in the water column (Eq. (20)). It can be obtained based on the diffusive flux S_c. Experimental measurements show that the release rate of nutrients is affected not only by the

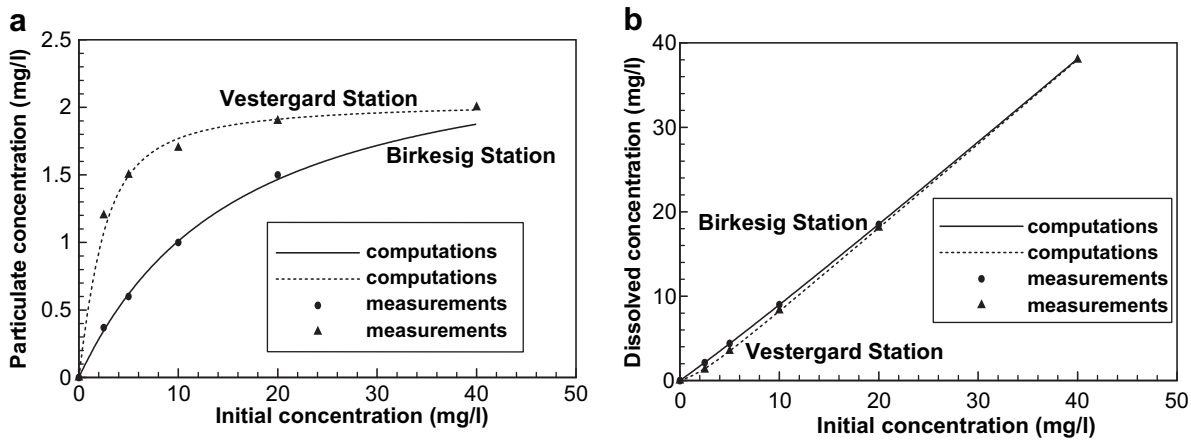

Fig. 1. Adsorption–desorption of phosphate by sediment at equilibrium. (a) The concentration of particulate phosphate versus different initial concentrations. (b) The concentration of dissolved phosphate versus different initial concentrations.

concentration gradient across the water–sediment interface, but also by the pH, temperature and DO. It is reported that the release rate of nutrient decreases with the increase of DO (Ishikawa and Nishmura, 1989; Kleeberg and Schlungbaum, 1993; Kim et al., 2003). In consideration of pH, it has been noted that under acidic conditions, the release rate decreases as pH increases, while under basic conditions, the release rate increases as pH increases (Kim et al., 2003; Fisher and Wood, 2004). Romero et al. (2003) proposed a formula to calculate the bed release rate S_{diff},which is consistent with measurements:

$$S_{\text{diff}} = \theta_{\text{sed}}^{T-20} S_{\text{c}} \left(\frac{K_{\text{dos}}}{K_{\text{dos}} + DO} + \frac{|\text{pH} - 7|}{K_{\text{pHs}} + |\text{pH} - 7|} \right) \tag{19}$$

where K_{dos} (mg/l)and K_{pHS} are the values that regulate the release of nutrient according to the DO and pH in the bottom layer of the water column of depth Δz_{b} (m); θ_{sed} is the temperature coefficient.

Eq. (19) was tested using a experiment designed to study the effect of pH on the phosphorus release rate at JSD Station in Han River (Kim et al., 2003). Fig. 2 shows the comparison between the computation results using Eq. (19) and experimental measurements. In general, the Eq. (19) provides reasonable predictions.

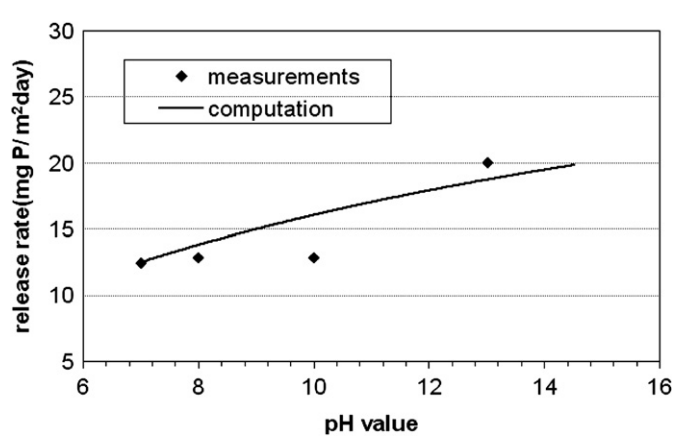

Fig. 2. Phosphorus release rate at JSD Station in Han River.

3. Numerical solution

3.1. Governing equations

In the water column, each one of the water quality constituents can be expressed by the following mass transport equation:

$$\frac{\partial C_{\text{i}}}{\partial t} + \frac{\partial (UC_{\text{i}})}{\partial x} + \frac{\partial (VC_{\text{i}})}{\partial y} + \frac{\partial (WC_{\text{i}})}{\partial z} = \frac{\partial}{\partial x}\left(D_{\text{x}} \frac{\partial C_{\text{i}}}{\partial x} \right) + \frac{\partial}{\partial y}\left(D_{\text{y}} \frac{\partial C_{\text{i}}}{\partial y} \right) + \frac{\partial}{\partial z}\left(D_{\text{z}} \frac{\partial C_{\text{i}}}{\partial z} \right) + \sum S_{\text{i}} \tag{20}$$

in which U, V, W are the water velocity components in x, y and z directions, respectively; C_{i} is the concentration of the ith water quality constituent; D_{x}, D_{y} and D_{z} are the diffusion coefficients in x, y and z directions, respectively; $\sum S_{\text{i}}$ is the effective source term, which includes the kinetic transformation rate, external loads and sinks for ith water quality constituent.

3.2. Numerical method

The proposed water quality model was decoupled with the CCHE3D hydrodynamic model (Jia et al., 2001). The CCHE3D model is based on the finite element method. As shown in Fig. 3, each element is a hexahedral with three levels of nine-node

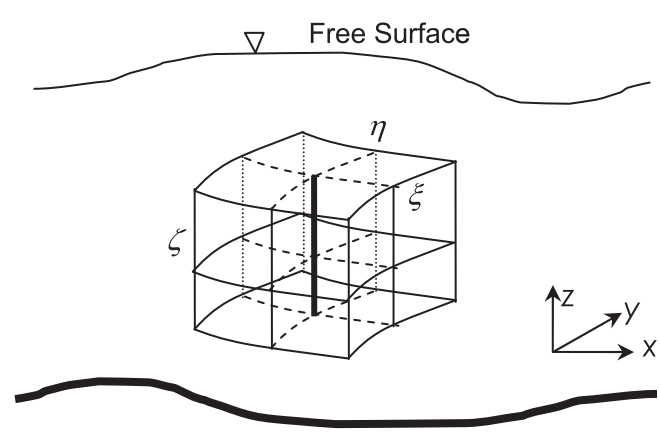

Fig. 3. Coordinate system and computational element. (In Fig. 3, the x, y,and z are axes of the Cartesian coordinate system and ξ, η and ζ are axes of a local system).

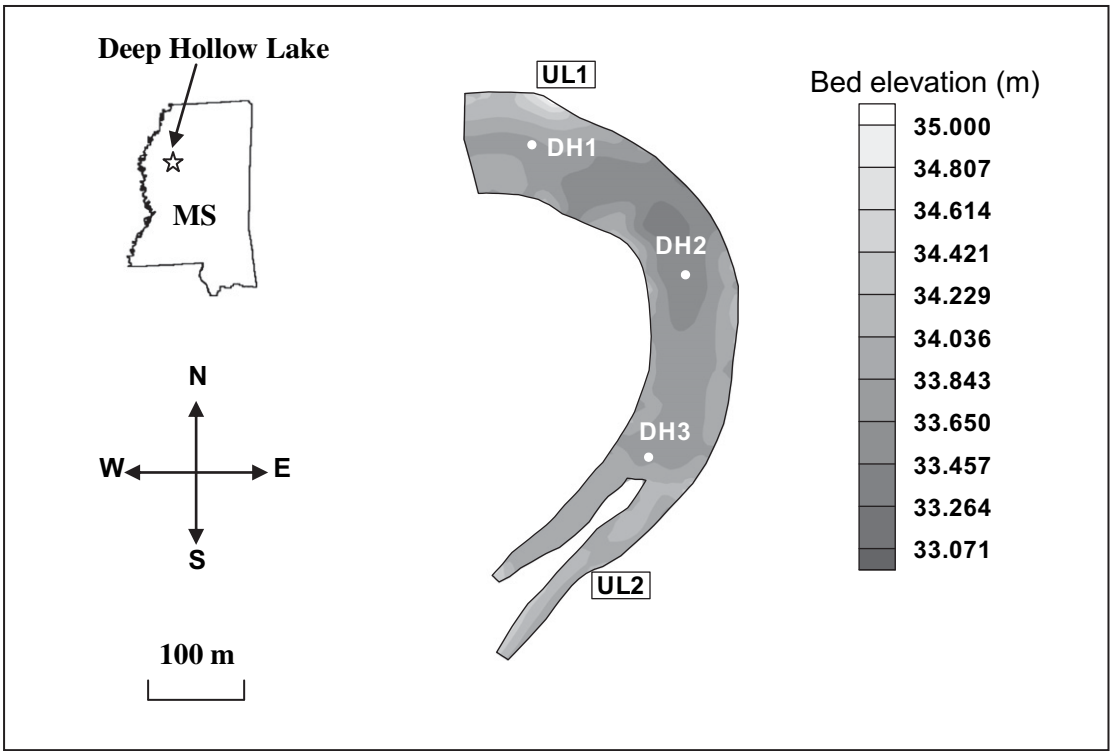

Fig. 4. Deep Hollow Lake.

quadrilaterals, and the governing equations are discretized using a 27-node hexahedral. The grid system in the horizontal plane is a structured conformal mesh generated on the boundary of the computational domain. The mesh lines are generally placed with finer resolution near the wall, bed and free surface.

A second-order upwinding scheme was adopted to eliminate oscillations due to advection. The velocity correction method was applied to solve the dynamic pressure and enforce mass conservation. Provisional velocities were solved first without the pressure term, and the final solution of the velocity was obtained by correcting the provisional velocities with the pressure solution (Jia et al., 2001). The system of algebraic equations was solved using the Strongly Implicit Procedure (SIP). Based on the flow fields computed by CCHE3D, the concentration distribution of water

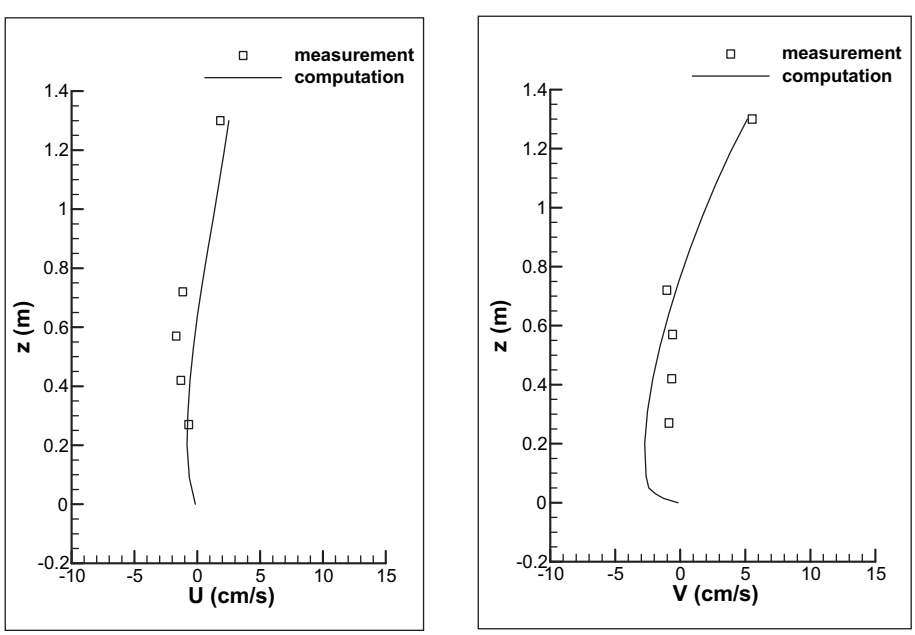

Fig. 5. Observed and simulated velocity at Station DH1 (11:05 am, 11/12/03).

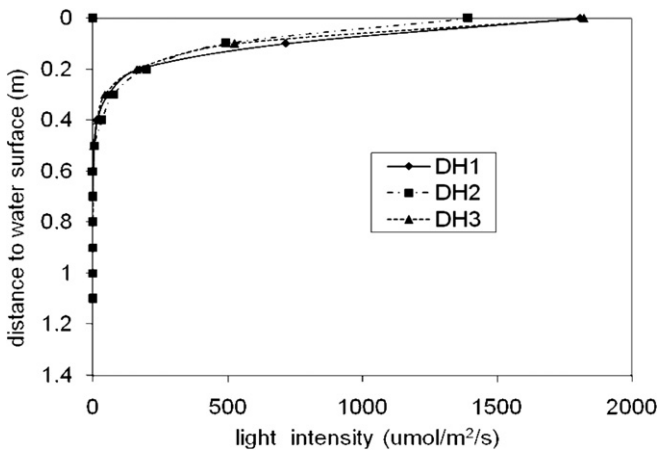

Fig. 6. Measured light intensity in water at DH1, DH2 and DH3 Stations (Jan.20, 2004).

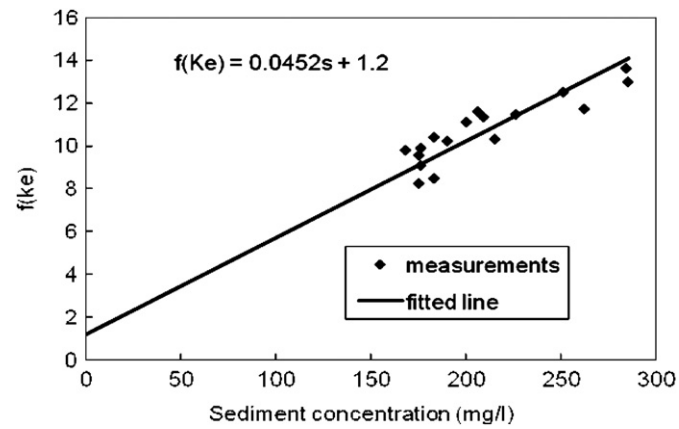

Fig. 8. Relationship between $f(k_e)$ and sediment concentration s.

quality constituents in water column can be obtained by solving mass transport Eq. (20) numerically.

4. Application to Deep Hollow Lake

4.1. Study area

Fig. 4 shows the study area of Deep Hollow Lake. It has a morphology typical of an oxbow lake, with a length of about 1 km and a width of about 100 m. Lake water depth ranges from 0.5 m to 2.6 m, with greatest depth in the middle. The lake receives runoff from a two square kilometer watershed that is heavily cultivated. This lake is located in Leflore County, Mississippi, and it was one of three natural lakes in the Mississippi River Alluvial Plain monitored under the interagency Mississippi Delta Management System Evaluation Area Project (MDMSEA). This project was part of a national program designed to evaluate the impact of agricultural production on water quality and to develop best management practices (BMPs) to minimize adverse effects of agricultural activities on water quality of the lakes (Nett et al., 2004).

Weekly or biweekly samples of SS, nutrients, chlorophyll, bacteria, and other selected water quality variables were collected at Stations DH1, DH2 and DH3. Two of the major inflows, located at the Stations UL1 and UL2, were monitored for water quality and quantity by the U.S. Geological Survey. The nutrient concentrations in Deep Hollow Lake are mainly dependent on the fertilizer loadings in the surrounding farmland and the quantity of runoff. Field measurements show that the concentrations of nitrate and ammonia in the lake are very low, while the concentration of phosphorus is relatively high in comparison with other areas nationwide. In this lake, pH varies from 6.5 to 7.5, and DO is always at the saturation level. The median diameter d_{50} of sediment particles in the lake is $\sim 2.5 \times 10^{-6}$–3×10^{-6} m, well within the clay size range. SS concentrations are relatively high, exceeding published levels known to adversely impact on fish growth and health (Rebich and Knight, 2001; Knight and Welch, 2004). Field data from stations DH1, DH2 and DH3 were used for model calibration and validation. In general, the data show that water quality conditions at the three stations were similar. Only the data from Station DH1 were presented in this study.

Based on bathymetric data, the computational domain was discretized into a structured finite element mesh using the CCHE Mesh Generator (Zhang, 2002). In the horizontal plane, the irregular computational domain was represented by a 95 × 20 mesh. In the vertical direction, the domain was divided into 8 levels with finer spacing near the bed. The bed sediment layer was represented by a 10 cm thick layer.

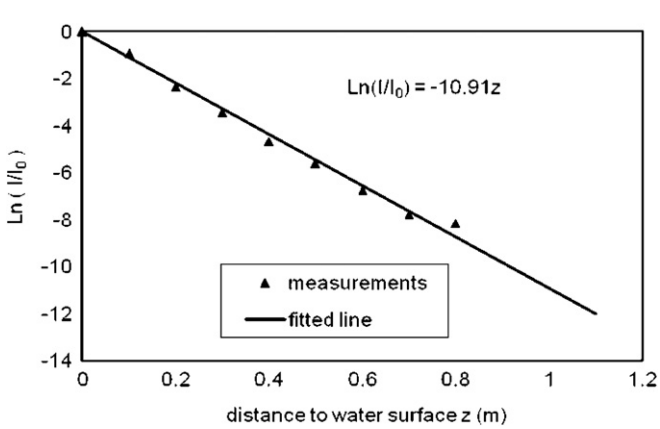

Fig. 7. $\ln(I/I_0)$ versus distance to water surface z at DH1 Station (Jan.20, 2004).

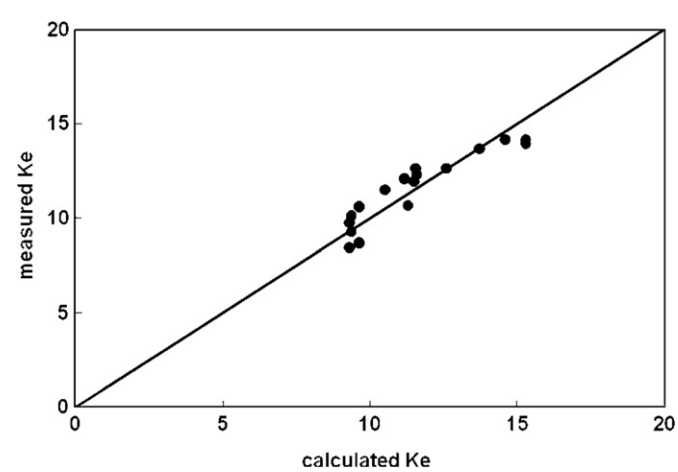

Fig. 9. Comparison of the light attenuation coefficient K_e obtained from Eq. (27) and field measurements.

Table 1
Some calibrated values of parameters for the water quality model applied to Deep Hollow Lake.

Parameter definition	Symbol	Value	Units
Maximum phytoplankton growth rate	P_{mx}	2.0	day^{-1}
Background light attenuation coefficient	K_0	1.2	m^{-1}
Light attenuation parameter related to SS	γ	0.0452	l/mg/m
Saturation light intensity of phytoplankton	I_m	300	ly/day
Half-saturation constant for nitrogen in phytoplankton growth	K_{mN}	0.01	mg/l
Half-saturation constant for phosphorus in phytoplankton growth	K_{mP}	0.001	mg/l
Effect coefficient of temperature below optimal temperature on growth	KTg_1	0.006	*none*
Effect coefficient of temperature above optimal temperature on growth	KTg_2	0.008	*none*
Ratio of adsorption and desorption rate coefficients for phosphorus	K	0.7	l/mg
Maximum adsorption capacity of phosphorus	Q_m	0.0051	mg P/mgSS
Diffusive exchange coefficient of phosphorus at water–sediment interface	k_p	0.01	mg/m^2day
Temperature coefficient	θ_{sed}	1.05	*none*
Control value of phosphorus release via DO	K_{pdos}	0.5	mg/l
Control value of phosphorus release via pH	K_{pH}	18	*none*

4.2. Model calibration and validation

The CCHE3D hydrodynamic model was first calibrated using field measurements obtained from Deep Hollow Lake using an Acoustic Doppler Current Profiler (ADCP), and then it was applied to simulate the flow field during the simulation period. Fig. 5 shows the comparison of simulated flow velocity with field measurements conducted on November 12, 2003. In general, numerical model provides good predictions for flow fields. After obtaining the flow fields, the concentrations of water quality constituents can be simulated using the proposed water quality model.

The water quality model was calibrated using field measurements obtained between April and June, 1999. For calibration runs, parameters in the water quality model were adjusted repeatedly to obtain a reasonable reproduction of the field data. Some of the model parameters were obtained directly from special experiments and field measurements, as described below and by others (Portielje and Lijklema, 1993; Cerco and Cole, 1995; DiToro, 2001; Wool et al., 2001; Hipsey et al., 2003; Bubba et al., 2003).

The light attenuation coefficient K_e in Eq. (10) is an important parameter for the growth of phytoplankton. To determine the parameters K_0 and γ in Eq. (10), about 20 sets of field measurements were conducted in Deep Hollow Lake to measure the light intensity,

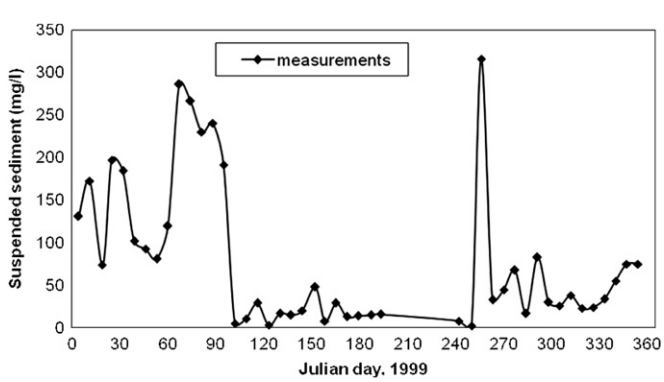

Fig. 10. Measured concentration of suspended sediment at Station DH1 (1999).

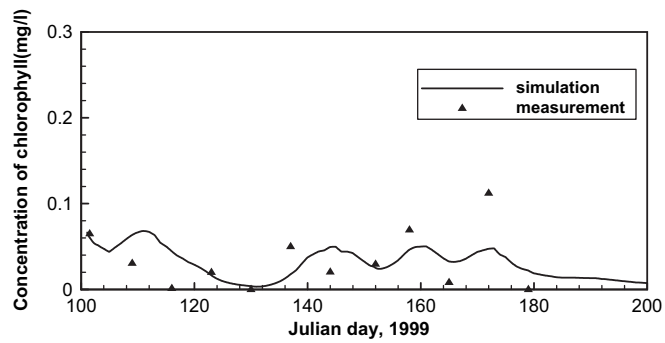

Fig. 11. The concentration of chlorophyll at Station DH1 (calibration).

and concentrations of suspended sediment and chlorophyll. The spatial variation of light down through the water column can be expressed as:

$$I = I_0 e^{(-K_e z)} \tag{21}$$

in which I is the light intensity; I_0 is the light intensity at the water surface; z is the distance of light travel through water. Eq. (21) can also be written as:

$$\ln\left(\frac{I}{I_0}\right) = -K_e z \tag{22}$$

So K_e can be obtained by linear fitting based on the measured I, I_0 and z.

Fig. 6 shows the measured light intensity under the water at DH1, DH2 and DH3 Stations. It can be observed that light intensity decreases quickly with the increase of depth in the water column due to the effects of water, sediment and phytoplankton. Light can penetrate about 1/3 of the total water depth. Fig. 7 clearly shows the linear relationship between $\ln(I/I_0)$ and the distance to the water surface z. The slope of the line is the measured light attenuation coefficient K_e (Eq. (22)).

Eq. (10) can also be expressed as

$$K_e - \left(0.0088C_{chl} + 0.054C_{chl}^{0.67}\right) = \gamma s + K_0 \tag{23}$$

set $f(K_e) = K_e - (0.0088C_{chl} + 0.054C_{chl}^{0.67})$, so

$$f(K_e) = K_e - \left(0.0088C_{chl} + 0.054C_{chl}^{0.67}\right) = \gamma s + K_0 \tag{24}$$

Based on the field data, a regression line, with the slope γ and intersection K_0 equal to 0.0452 and 1.2, respectively, was obtained (Fig. 8). So Eq. (10) can be written as

$$K_e = 1.2 + 0.0088C_{chl} + 0.054C_{chl}^{0.67} + 0.0452s \tag{25}$$

Eq. (25) was adopted to calculate the light attenuation coefficient in Deep Hollow Lake. Fig. 9 compares the light attenuation coefficient K_e obtained from field measurements and calculations from Eq. (25). Good agreement was obtained with an r^2 value of 0.86.

Field measurements indicated that the concentrations of ammonium and nitrate in Deep Hollow Lake were very low, so the adsorption and desorption of ammonium and nitrate from sediment were expected to be insignificant and were not incorporated. At equilibrium, the concentration of dissolved and particulate phosphate due to adsorption–desorption was calculated using Eqs. (16) and (17). Dissolved inorganic and organic nutrients may also be released to the water column from bed sediments. In the water

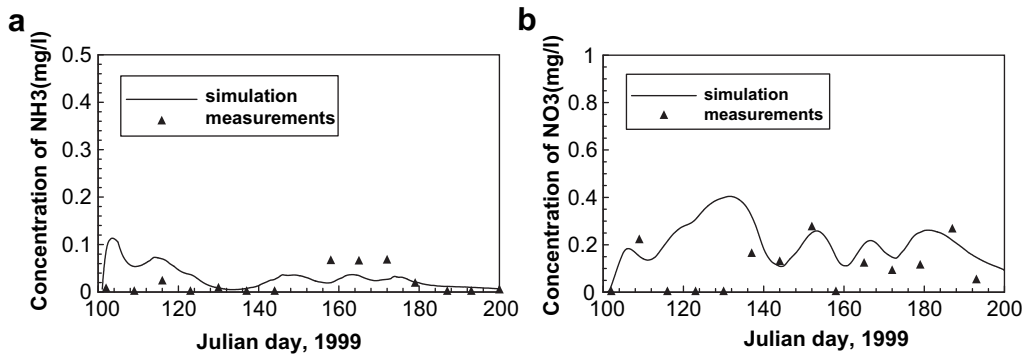

Fig. 12. The concentration of nitrogen at Station DH1 (calibration). (a) Concentration of NH3. (b) Concentration of NO3.

quality model, the bed release rate of ammonium, nitrate, organic nitrogen, phosphate, and organic phosphorus were calculated using Eq. (19). Reported data from laboratory experiments and field measurements were used to generate the necessary parameters for simulating the processes of adsorption–desorption and bed release when Deep Hollow data were not available (Portielje and Lijklema, 1993; Appan and Wang, 2000; DiToro, 2001; Wool et al., 2001; Hipsey et al., 2003; Bubba et al., 2003; Kim et al., 2003). Some calibrated parameters related to sediment-associated water quality processes are listed in Table 1.

In the numerical model, the measured water temperature, surface light intensity, suspended sediment concentration, and pH were set as input data. Fig. 10 shows the measured concentration of suspended sediment at Station DH1. The model calibration results of chlorophyll, nitrogen and phosphorus for Station DH1 are shown in Figs. 11, 12 and 13, respectively. In general, the model provided reasonable reproduction of patterns and acceptable magnitudes for water quality constituents. The mean values of the model results are generally in good agreement with the field observations. However, the ability of the model to reproduce temporal variations in field measurements was not as good as the mean values. Those differences may arise due to the fact that measurements occurred weekly while the time step for the simulation was 1 h. In addition, the water quality processes in the lake system are likely more complicated than those reproduced in the simulation model.

The period from September to December 1999 was chosen for model validation. Computed flow currents, and measured boundary conditions, weather data and SS concentrations were used to predict the concentrations of water quality constituents. Parameter values in the water quality model were those calibrated values using the data of April–June 1999. Figs. 14 and 15 show the simulated and observed concentrations of chlorophyll and nitrogen. Similar to the calibration runs, trends and quantities of concentration of chlorophyll and nitrogen obtained from the numerical model were generally in agreement with the observations. Fig. 16a and b show the simulated and observed concentrations of ortho-phosphorus and organic phosphorus, respectively. It can be seen the numerical results are generally in good agreement with field measurements after considering the sediment related water quality processes.

5. Discussions

5.1. Comparison of Langmuir equation and linear approach for simulating the processes of adsorption–desorption

In many water quality models, both the Langmuir equation and the linear approach have been applied to simulate the processes of adsorption–desorption (Delft Hydraulics, 2003; Wool et al., 2001; Cerco and Cole, 1995; Smits and Molen, 1993). For the linear approach, the adsorption–desorption of nutrients by sediment is described by a linear isotherm, and the equilibrium adsorption concentration Q (mg/mg SS) can be expressed as

$$Q = K_p C_d \tag{26}$$

in which K_p is the partition coefficient. Based on Eqs. (13), (14) and (26), C_p and C_d can be calculated by

$$C_p = \frac{K_p s}{1 + K_p s} C_0 \tag{27}$$

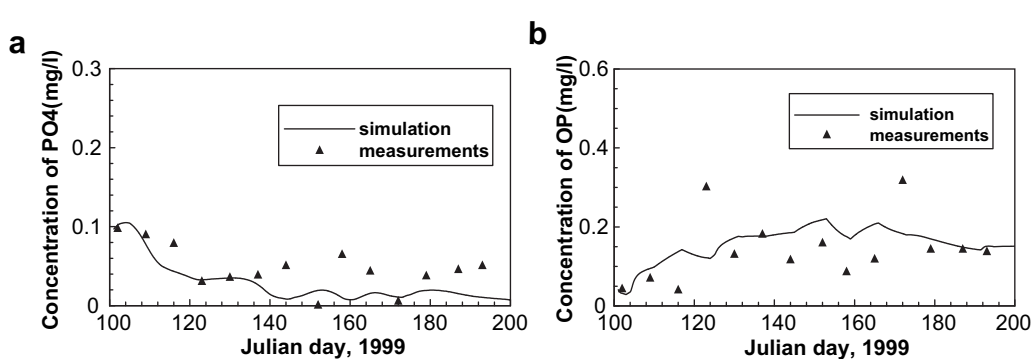

Fig. 13. The concentration of phosphorus at Station DH1 (calibration). (a) Concentration of PO4. (b) Concentration of OP.

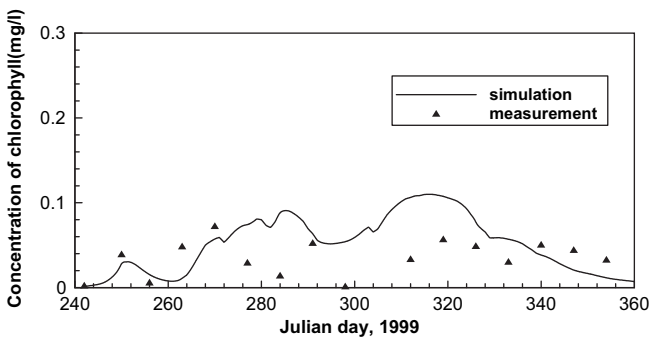

Fig. 14. The concentration of chlorophyll at Station DH1 (validation).

$$C_d = \frac{1}{1 + K_p s} C_0 \tag{28}$$

Eqs. (27) and (28) have been used in some water quality models for calculating the particulate and dissolved nutrient concentrations at each time step due to adsorption–desorption based on the linear approach. In fact, this approach is satisfactory only when nutrient concentrations are low (Chapra, 1997). If the nutrient concentration is very low, the term $(1 + KC_d)$ in Langmuir equation (Eq. (11)) approximately equals to 1, so Eq. (11) can be simplified as:

$$Q = Q_m K C_d \tag{29}$$

which implies that the partition coefficient

$$K_p = Q_m K \tag{30}$$

and then Eq. (29) is same as the linear approach Eq. (26). So Eq. (26) is the linear portion of the Langmuir equation. In order to find a maximum nutrient concentration (upper bound) for adopting the linear approach, Eqs (27), (28) and (16), (17) were used to calculate the particulate and dissolved concentrations of nutrients in Deep Hollow Lake due to adsorption–desorption. For the Deep Hollow Lake case, the Langmuir adsorption constant K and the maximum adsorption capacity Q_m were taken as 0.7 l/mg and 0.0051 mg/mg SS, respectively. If the linear approach was adopted, based on Eq. (30), the partition coefficient K_p is 0.00357 l/mg. Fig. 17a and b show the concentrations of particulate and dissolved phosphate calculated based on the linear approach (Eqs. 27 and 28) and the Langmuir equation (Eqs. 16 and 17) under different initial concentrations. It can be observed that the linear approach and the Langmuir equation have same results if the initial concentration is less than 0.1 mg/l. In Deep Hollow Lake, the phosphate concentration can be greater than 0.3 mg/l, so the Langmuir equation is more appropriate.

5.2. Effect of sediment on the phosphorus concentration

The effects of sediment adsorption–desorption and bed release play important roles in phosphorus cycles of natural water body. The simulated concentrations of phosphate and organic phosphorus were compared with field observations and simulation results without considering the effects of sediment. As shown in Fig. 16a and b, without considering the sediment-associated processes of adsorption, desorption and bed release, the model overestimates phosphate concentration and underestimates organic phosphorus. After considering those processes, the RMSEs of phosphate and organic phosphorus concentration reduce from 0.029 to 0.016 mg/L, and from 0.051 to 0.037 mg/L, respectively.

5.3. Sensitivity of chlorophyll concentration to SS

Field data show that major water quality problems in Deep Hollow Lake were caused by excessive sediment loads carried by runoff from surrounding cultivated lands in the late 1990s. In order to improve the water quality of the lake, various best management practices (BMPs), such as edge-of-field BMPs and agronomic BMPs were employed to reduce sediment loads entering the lake from cultivated fields. After the reduction of lake sediment concentration, there were significant increases in Secchi depth and chlorophyll concentration, and fish populations responded positively (Rebich and Knight, 2001).

To show the sensitivity of chlorophyll concentration to SS, a series of hypothetical lake SS concentrations were input to the model, while the flow conditions and nutrient loadings at inlet boundaries were kept the same. The interactions between SS and nutrients in the lake were considered in the model simulation. The calibration and validation periods were selected for sensitivity study. SS levels were varied from 10% to 300% of the current sediment condition, and the model was applied to simulate the response of chlorophyll concentration in the lake. As expected, the concentration of chlorophyll is inversely related to sediment concentration. Fig. 18 shows the sensitivity of temporal mean chlorophyll concentration to SS for the entire simulation period at Station DH1. In this figure, the square represents the base condition (SS = 100%, Chlorophyll = 100%). When lake SS was reduced by 50%, simulated mean chlorophyll concentration increased about 40%. When lake SS was doubled, the chlorophyll concentration fell to 37% of the base condition. Field observations of SS and chlorophyll

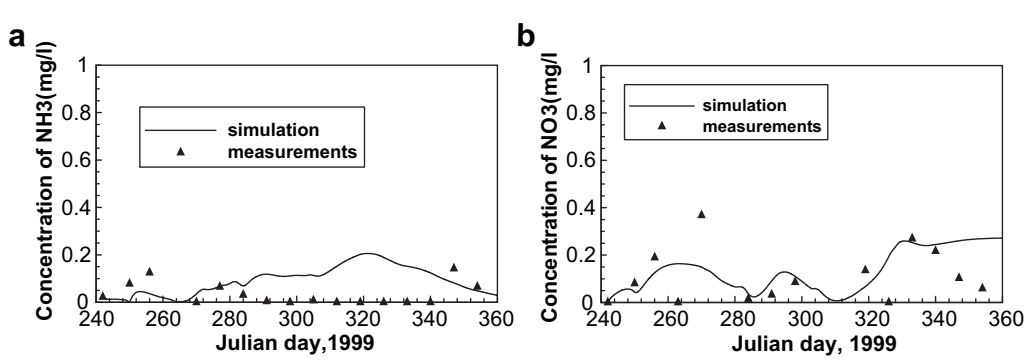

Fig. 15. The concentration of nitrogen at Station DH1 (validation). (a) Concentration of NH3. (b) Concentration of NO3.

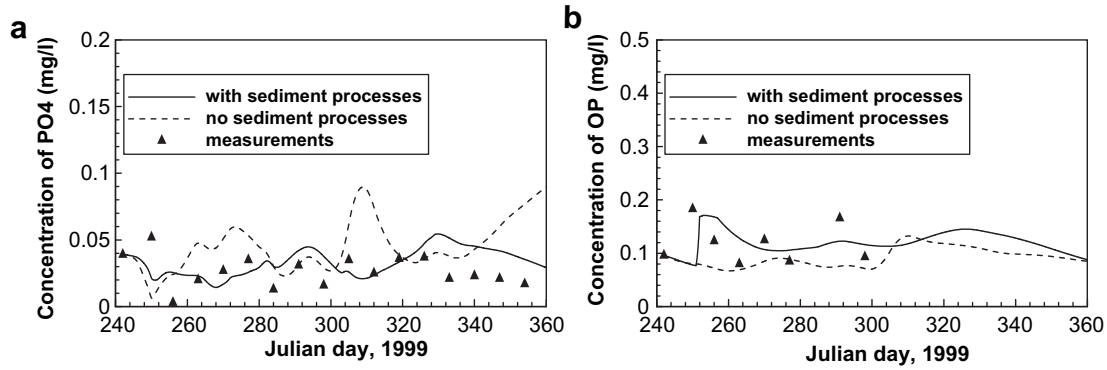

Fig. 16. The concentration of phosphorus at Station DH1 (validation). (a) Concentration of PO4. (b) Concentration of OP.

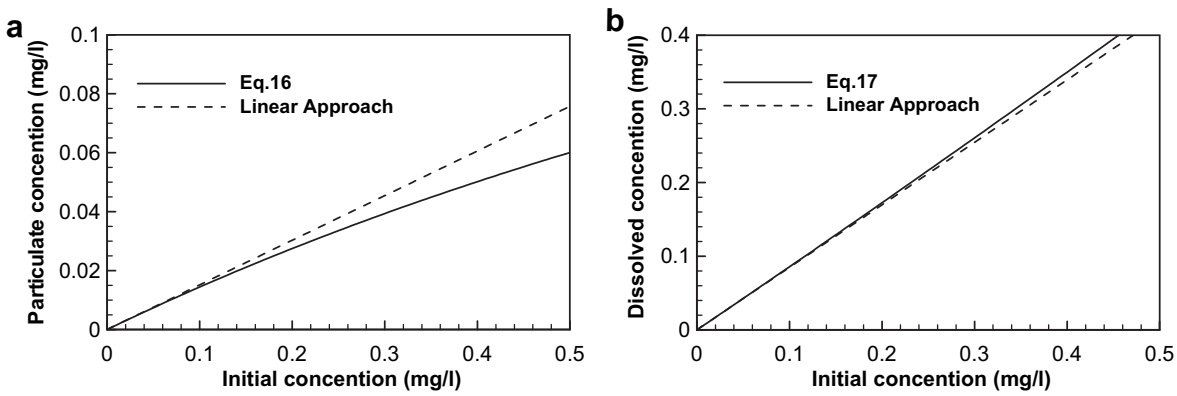

Fig. 17. Comparison of particulate and dissolved phosphate concentrations obtained based on the Linear approach and Langmuir equation. (a) Particulate concentration. (b) Dissolved concentration.

in the years 1999, 2000 and 2001 were used to evaluate the model sensitivity analysis. Measured mean concentrations of SS and chlorophyll under the base condition (Year 1999) were 82 mg/L and 40 mg/L, respectively. Mean concentrations of SS in 2000 and 2001 were reduced to 56% and 62% of base condition, and the chlorophyll concentrations increased to 142% and 137% of the base condition, respectively. The numerical results described above are in agreement with these measurements (Fig. 18).

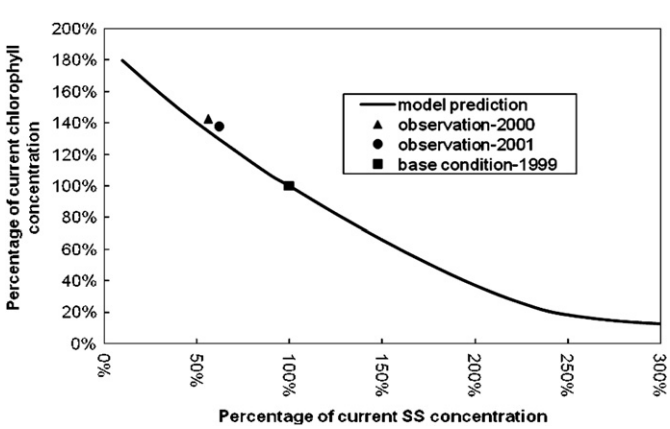

Fig. 18. Sensitivity of temporal mean chlorophyll concentration to temporal mean SS.

6. Conclusions

A three-dimensional numerical model was developed to simulate the concentrations of water quality constituents in shallow natural lakes where sediment-associated water quality processes are important. Four biochemical cycles were simulated, and eight state variables were involved in the interacting systems. Sediment-associated processes in the water quality model were studied. A formula was obtained from field measurements to calculate the effect of suspended sediment on the light attenuation coefficient (Eq. (25)). Based on the Langmuir equation, two algebraic Eqs. (16) and (17) were derived to calculate the equilibrium concentrations of particulate and dissolved nutrients due to adsorption–desorption. A formula (Eq. (19)) was obtained to calculate the release rate from bed sediment by considering the effects of the concentration gradient across the water–sediment interface, pH, temperature and DO concentration.

The model was successfully applied to the study of the concentration of constituents important to the water quality of the Deep Hollow Lake. Realistic trends and magnitudes of nutrient and phytoplankton concentrations obtained from the numerical model generally agreed with field observations. The effects of sediment-associated processes are quite important in water quality processes. Without considering the sediment-associated processes, the model overestimated ortho-phosphorus concentration and underestimated organic phosphorus. After considering those processes, the numerical results show better agreements with field observations.

The model was also used to conduct analyses of the sensitivity of lake chlorophyll concentration to concentrations of suspended sediment. Lake primary productivity is mainly limited by suspended sediment concentration, which limits light penetration. Since the water quality and ecology of shallow lakes receiving agricultural runoff are governed by agricultural practices, the model presented here may be applied to assess effects of conservation measures.

Acknowledgements

This study is part of the research project sponsored by the USDA-ARS Specific Research Agreement No. 58-6408-7-236 (monitored by the USDA-ARS National Sedimentation Laboratory) and the University of Mississippi. The suggestions and advice provided by Dr. Tingting Zhu and Dr. Weiming Wu of the University of Mississippi are highly appreciated.

References

Appan, A., Wang, H., 2000. Sorption isotherms and kinetics of sediment phosphorus in a tropical reservoir. Journal of Environmental Engineering 126, 993–998.
Bubba, M.D., Arias, C.A., Brix, H., 2003. Phosphorus adsorption maximum of sands for use as media in subsurface flow constructed reed beds as measured by the Langmuir isotherm. Water Research 37, 3390–3400.
Cerco, C.F., Cole, T., 1995. User's Guide to the CE-QUAL-ICM: Three-Dimensional Eutrophication Model. Technical Report EL-95–1 5. U.S. Army Corps of Engineers, Vicksburg, MS.
Chapra, S.C., 1997. Surface Water-Quality Modeling. The Mcgraw-Hill Companies, Inc, New York.
Chung, S.W., Ko, I.H., Kim, Y.K., 2008. Effect of reservoir flushing on downstream river water quality. Journal of Environmental Management 86 (1), 139–147.
Danish Hydraulic Institute, 2005. Coastal and Inland waters in 3D. http://www.dhi.dk (Jan 2005).
Delft Hydraulics, 2003. "Delft3D-WAQ: Technical Reference Manual". WL | Delft Hydraulics, The Netherlands.
DiToro, 2001. Sediment Flux Modeling. Wiley-Interscience, New York.
Dortch, M.S., Zakikhani, M., Kim, S.C., Steevens, J.A., 2008. Modeling water and sediment contamination of Lake Pontchartrain following pump-out of Hurricane Katrina floodwater. Journal of Environmental Management 87 (3), 429–442.
Fan, C., Ko, C.H., Wang, W.S., 2009. An innovative modeling approach using Qual2K and HEC-RAS integration to assess the impact of tidal effect on River Water quality simulation. Journal of Environmental Management 90 (5), 1824–1832.
Fisher, L.H. and Wood, T.M., 2004. "Effect of water-column pH on sediment-phosphorus release rate in upper Klamath Lake, Oregon, 2001", USGS water Resources Investigation Report 03–4271.
Fox, I., Malati, M.A., Perry, R., 1989. The adsorption and release of phosphate from sediment of a river receiving sewage effluent. Water Research 23, 725–732.
Gin, K.Y.H., Zhang, Q.Y., Chan, E.S., Chou, L.M., 2001. Three-dimensional ecological-eutrophication model for Singapore. Journal of Environmental Engineering 127, 928–937.
Hipsey, M.R., et al., 2003. Computational Aquatic Ecosystem Dynamics Model: CAEDYM V2, User Manual. University of Western Australia.
Hydroqual, 2004. User's Guide for RCA, Release 3.0. Hydroqual, Inc, New Jersey.
Ishikawa, M., Nishmura, H., 1989. Mathematical model of phosphate release rate from sediment considering the effect of dissolved oxygen in overlying water. Water Research 23, 351–359.
Jia, Y., Kitamura, T., Wang, S.S.Y., 2001. Simulation of scour process in plunge pool of loose bed-material. Journal of Hydraulic Engineering 127, 219–229.
Jin, K.R., James, R.T., Lung, W.S., Loucks, D.P., Park, R.A., Tisdale, T.S., 1998. Assessing lake Okeechobee eutrophication with water-quality models. Journal of Water Resources Planning and Management 124, 22–30.
Kim, L.H., Choi, E., Stenstrom, M.K., 2003. Sediment characteristics, phosphorus types and phosphorus release rates between river and lake sediments. Chemosphere 50 (1), 53–61.
Kleeberg, A., Schlungbaum, G., 1993. In situ phosphorus release experiments in the Warnow River (Mecklenburg, northern Germany). Hydrobiologia 253, 263–274.
Knight, S.S., Welch, T.D., 2004. Evaluation of watershed management practices on oxbow lake ecology and water quality. In: in Nett, M.T., Locke, M.A., Pennington, D.A. (Eds.), Water Quality Assessments in the Mississippi Delta. ACS Symposium Series 877. American Chemical Society, Washington, DC.
Kuo, J.T., Hsieh, P.H., Jou, W.S., 2008. Lake eutrophication management modeling using dynamic programming. Journal of Environmental Management 88 (4), 677–687.
Loeff, M.R., et al., 1984. The asphyxiation technique: an approach to distinguishing between molecular diffusion and biologically mediated transport at the sediment–water interface. Limnology and Oceanography 29, 675–686.
Moore, P.A., Reddy, K.R., Fisher, M.M., 1998. Phosphorus flux between sediment and overlying water in Lake Okeechobee, Florida: spatial and temporal variations. Journal of Environmental Quality 27, 1428–1439.
Nett, M.T., Locke, M.A., Pennington, D.A., 2004. Water Quality Assessments in the Mississippi Delta. In: ACS Symposium Series 877. American Chemical Society, Washington, DC.
Portielje, R., Lijklema, L., 1993. Sorption of phosphate by sediment as a result of enhanced external loading. Hydrobiologia 253, 249–261.
Rebich, R.A., Knight, S.S., 2001. The Mississippi Delta Management Systems Evaluation Area Project, 1995–99. Mississippi Agriculture and Forestry Experiment Station, Information Bulletin 377. Division of Agriculture, Forestry and Veterinary Medicine, Mississippi State University.
Romero, J.R., et al., 2003. Computational Aquatic Ecosystem Dynamics Model: CAEDYM V2, Science Manual. University of Western Australia.
Smits, J.G.C., Molen, D.T., 1993. Application of SWITCH, a model for sediment-water exchange of nutrients, to Lake Veluwe in the Netherlands. Hydrobiologia 253, 281–300.
Stefan, H.G., et al., 1983. Model of light penetration in a turbid lake. Water Resources Research 19 (No. 1), 109–120.
Wool, T.M., et al., 2001. Water Quality Analysis Simulation Program (WASP) Version 6 User's Manual. US Environmental Protection Agency, Atlanta, GA.
Zhang, Y.X., 2002. CCHE Mesh Generator User Manual, Technical Report. The University of Mississippi.